ARTICLE OPEN

Ensembles of climate simulations to anticipate worst case heatwaves during the Paris 2024 Olympics

Pascal Yiou [1✉], Camille Cadiou[1], Davide Faranda [1,2,3], Aglaé Jézéquel[3,4], Nemo Malhomme[1], George Miloshevich[1], Robin Noyelle[1], Flavio Pons [1], Yoann Robin[1] and Mathieu Vrac [1]

The Summer Olympic Games in 2024 will take place during the apex of the temperature seasonal cycle in the Paris Area. The mid-latitudes of the Northern hemisphere have witnessed a few intense heatwaves since the 2003 event. Those heatwaves have had environmental and health impacts, which often came as surprises. In this paper, we search for the most extreme heatwaves in Ile-de-France that are physically plausible, under climate change scenarios, for the decades around 2024. We circumvent the sampling limitation by applying a rare event algorithm on CMIP6 data to evaluate the range of such extremes. We find that the 2003 record can be exceeded by more than 4 °C in Ile-de-France before 2050, with a combination of prevailing anticyclonic conditions and cut-off lows. This study intends to raise awareness of those unprecedented events, against which our societies are ill-prepared, in spite of adaptation measures designed from previous events. Those results could be extended to other areas of the world.

INTRODUCTION

Summer heatwaves in the northern midlatitudes have lead to many impacts on society and ecosystems, since the major event that struck Western Europe in 2003[1]. Since that epitome event, nations have taken measures to mitigate the effects of such extremes, especially on public health[2] and energy[3]. Climate model projections have suggested that the records of the early 21st century could be regularly broken in the second part of the 21st century[4].

The Olympic games in 2024 will take place in Paris between July 26th and August 10th, which is at the apex of the temperature seasonal cycle. During that event, it is expected that tens of thousands of visitors from the whole world will stay outdoors, and be exposed to potential heat stress. As shown in Fig. 1a, the preceding summer Olympics in Tokyo (2021) were the warmest on record since 1952, with an average temperature that exceeded the value in Paris in 2003. The Tokyo heatwave had a huge impact on the athletes and volunteers during outdoor competitions[5]. Health impacts on the public had been anticipated[6,7], but the COVID crisis limited the foreign public exposure in 2021. The previous Olympic games were organized at different periods of the year and in different hemispheres, but the temperatures yield a generally increasing trend (triangles in Fig. 1a).

Anticipating the risks of an intense heatwave in the present decades, i.e. a worst case scenario, is crucial for society. The field of Extreme Event Attribution (EEA[8]) has built concepts and methods to evaluate if and how climate change has altered the probabilities of extreme events. Many of the results of EEA rely on ensembles of physical or statistical model simulations. A recently developed approach to gain numerical efficiency has applied rare event algorithms[9] that nudge trajectories towards extreme values. This approach allows simulating the most extreme events, without having to consider most "normal" events. So far, this approach has been based on single model experiments[9,10] or constrained by reanalysis data[11]. Both studies focused on present-day or pre-industrial conditions. Therefore there is an urgent need

to apply this type of method to scenarios of climate change, in order to evaluate worst cases in near future climate conditions.

We consider mean daily temperature (TG) and determine the warmest period of 15 days (in Ile-de-France) in July-August, for each year (TG15d). This length (15 days) is motivated by the duration of Olympic games. The goal of this paper is to estimate worst case scenarios of TG15d heatwaves in the Paris area in the decades around 2024, and outline the synoptic features of those events in order to understand whether their causes are unique. The strategy is to use a stochastic model constrained by the atmospheric circulation, so-called Stochastic Weather Generator (SWG)[12,13], to simulate large ensembles of extreme heatwaves that are consistent with state-of-the-art climate models. This stochastic model will consider four scenarios for climate change (SSP1-2.6, SSP2-4.5, SSP3-7.0, SSP5-8.5) and a panel of coupled climate model simulations as input (see Section Experimental set-up of simulations). We use a set of 14 CMIP6 model simulations[14] to sample the model dependence of the simulation of extreme heatwaves. A state-of-the-art bias correction method[15] is applied, so that the main statistics of the present-day model simulations are close to observations. In order to build robustness, a statistical analysis of extremes[16] allows estimating the probabilities of extreme events, and their dependence on the emission scenarios. The methods and data are described in the Methods section.

RESULTS

Heatwaves in CMIP6 and ERA5

Temperature time series of the warmest 15-day periods (TG15d) in July-August in Ile-de-France are shown in Fig. 1a, for the IPSL climate model (one simulation for each scenario). As anticipated by the bias correction procedure, the temperature variability is similar to the ERA5 reanalysis[17] variability for all models (Fig. 1a, b). In the IPSL model, the July-August average summer temperature increases by ≈ 1.6 to ≈ 2.1 °C from 1951–2000 to 2001–2050, depending on the scenario (not shown). The average TG15d

[1]Laboratoire des Sciences du Climat et de l'Environnement, UMR 8212 CEA-CNRS-UVSQ, IPSL & U Paris-Saclay, Gif-sur-Yvette, France. [2]London Mathematical Laboratory, London, UK. [3]Laboratoire de Météorologie Dynamique, UMR CNRS-ENS-X, Paris, France. [4]Ecole des Ponts Paristech, Champs-sur-Marne, France. ✉email: pascal.yiou@lsce.ipsl.fr
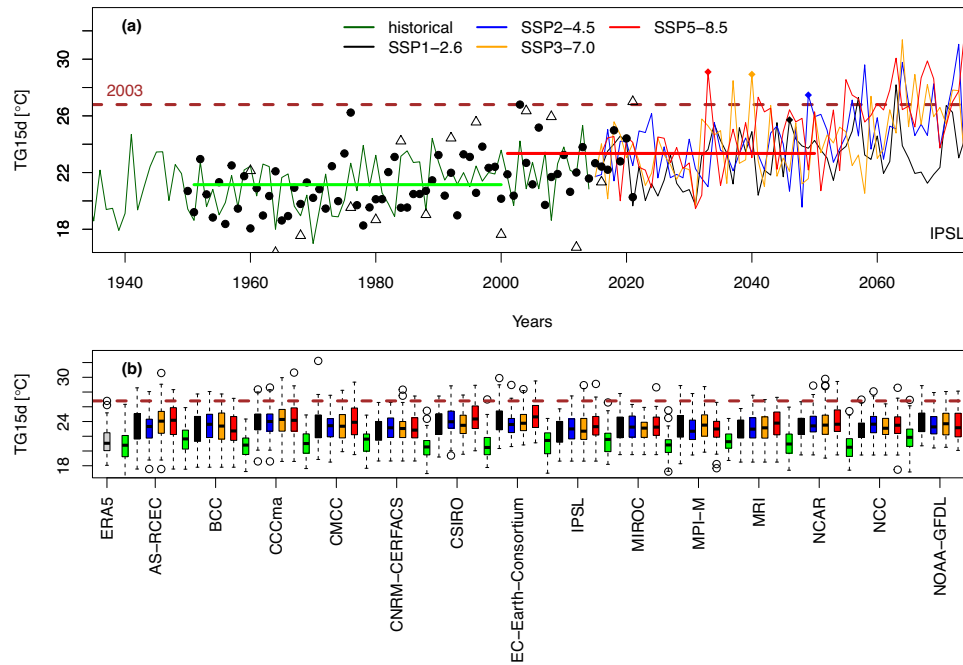
Fig. 1 Variations of TG15d in CMIP6 simulations and the ERA5 reanalysis. Panel **a**: Time series of TG15d (July-August) in Ile-de-France. The values correspond to the IPSL model simulations with four SSP scenarios. The dark green line is for the historical period (1900–2014). The circles represent TG15d variations in the ERA5 reanalysis. The triangles represent the 15-day average temperature (from the ERA5 reanalysis) during the preceding Olympics, in each organizing city, since 1952 (the temperatures during the summer Olympics in 1952 and 1956 were lower than 15 °C). The two horizontal bars represent the average over the two key periods (1951–2000: green; 2001–2050: red for SSP5-8.5). Diamonds outline the warmest TG15d values in 2001–2050 for the four scenarios. Panel **b**: boxplots of TG15d over Ile-de-France for each model and each SSP scenario. The gray boxplot on the left is for ERA5 (1950–2021). Green boxplots are for 1951–2000. black, blue, orange, and red boxplots are for 2001–2050, with the SSP1-2.6, SSP2-4.5, SSP3-7.0, and SSP5-8.5 scenarios, respectively. The boxes of boxplots indicate the median ($q50$), the lower and upper hinges indicate the 25th ($q25$) and 75th ($q75$) quantiles. The upper whiskers indicate $\min[\max(\text{TG15d}), q50 + 1.5 \times (q75 - q25)]$. The lower whisker has a symmetric formulation. The horizontal brown dashed line is the 2003 value (TG15d = 26.8 °C) in ERA5.

increases by ≈ 1.4 to $\approx 2.2\,°C$ (Fig. 1a) over the same period, depending on the SSP scenario. The differences in the maximum TG15d between those two periods range from 1.8 to 3.5 °C in the IPSL model, depending on the scenario. The largest difference is obtained for SSP2-4.5. Therefore, the mean July-August and TG15d show a similar mean increase, while the maximum values of TG15d yield a larger increase for this model.

We summarize the variability range of TG15d in CMIP6 simulations in Fig. 1b. This illustrates the most extreme values that can be reached with this multi-model ensemble, under the four SSP scenarios. This shows that bias corrected CMIP6 simulations sample the variability of temperature obtained by ERA5 reanalysis in the historical period. A Kolmogorov-Smirnov test cannot detect differences between the empirical probability distributions of TG15d in four CMIP6 SSP scenario simulations between 2001 and 2050. The most extreme values of TG15d in 2001-2050 (in CMIP6 data) are not necessarily detected in SSP5-8.5 simulations, because the scenario simulations are barely distinguishable before 2050. The observed record value (in ERA5) for the summer warmest 15 days in 2003 (26.8 °C) is never exceeded in the 20th century in CMIP6 simulations (green boxplots in Fig. 1b), and is occasionally exceeded (less than 10% time) in 2001–2050. This plot motivates the simulation of events that are close to the upper limit of those known values (Fig. 1b), as the mean temperature increase (over the whole season or TG15d) between 1951–2000 and 2001–2050 is likely to increase the probability of breaking the 2003 record.

Stochastic simulations of heatwaves from IPSL model data

We illustrate SWG simulations of extreme events (see section Stochastic weather generator (SWG) and importance sampling)

with data from the IPSL model with four SSP scenarios. We compare 15-day SWG simulations starting the first day of the TG15d identified in Fig. 1a in 2001–2050 for the four SSP scenarios. The initial conditions depend on the years because TG15d can occur between the 1st of July and the 31st of August, and the SSP scenarios. Hence we show how the extremes simulated with the SWG depend on the reference period of analogs (1951–2000 vs. 2001–2050).

The probability distribution of all TG15d values slightly changes with SSP scenarios (similar medians and non-significant Kolmogorov–Smirnov tests on the horizontal lines in Fig. 2). The record 2003 value is exceeded in the three "intense" SSP scenarios, although not in SSP1-2.6, with this IPSL model simulation. The highest values for TG15d can occur with any scenario when considering the CMIP6 ensemble (not shown).

These results with SWG simulations from the IPSL model data (boxplots in Fig. 2a–d) show that the temperature increase of the most extreme events between 1951–2000 and 2001–2050 exceeds 3.5 °C in three SSP scenario simulations (from SSP2-4.5, SSP3-7.0, and SSP5-8.5). More than half of the SWG heatwaves with analogs in 1951-2000 stand above the upper half of the TG15d values in 2001–2050 (above the median), but not the outliers (Fig. 2a). The value observed in 2003 (in ERA5) is not reached with SWG simulations from the IPSL model and analogs in 1951–2000. The 2003 observed record (red dash-dotted lines in Fig. 2) is exceeded by a large margin in SSP2-4.5, SSP3-7.0, and SSP5-8.5 scenarios (orange lines vs. brown lines in Fig. 2 (top panels)), between 2040 and 2050, although it is still a rare value in 2001–2050. The most intense TG15d heatwaves detected in the IPSL model data (orange dashed lines) can be exceeded by 1 °C or with probability that exceeds 25% (upper whiskers in Fig. 2b) with
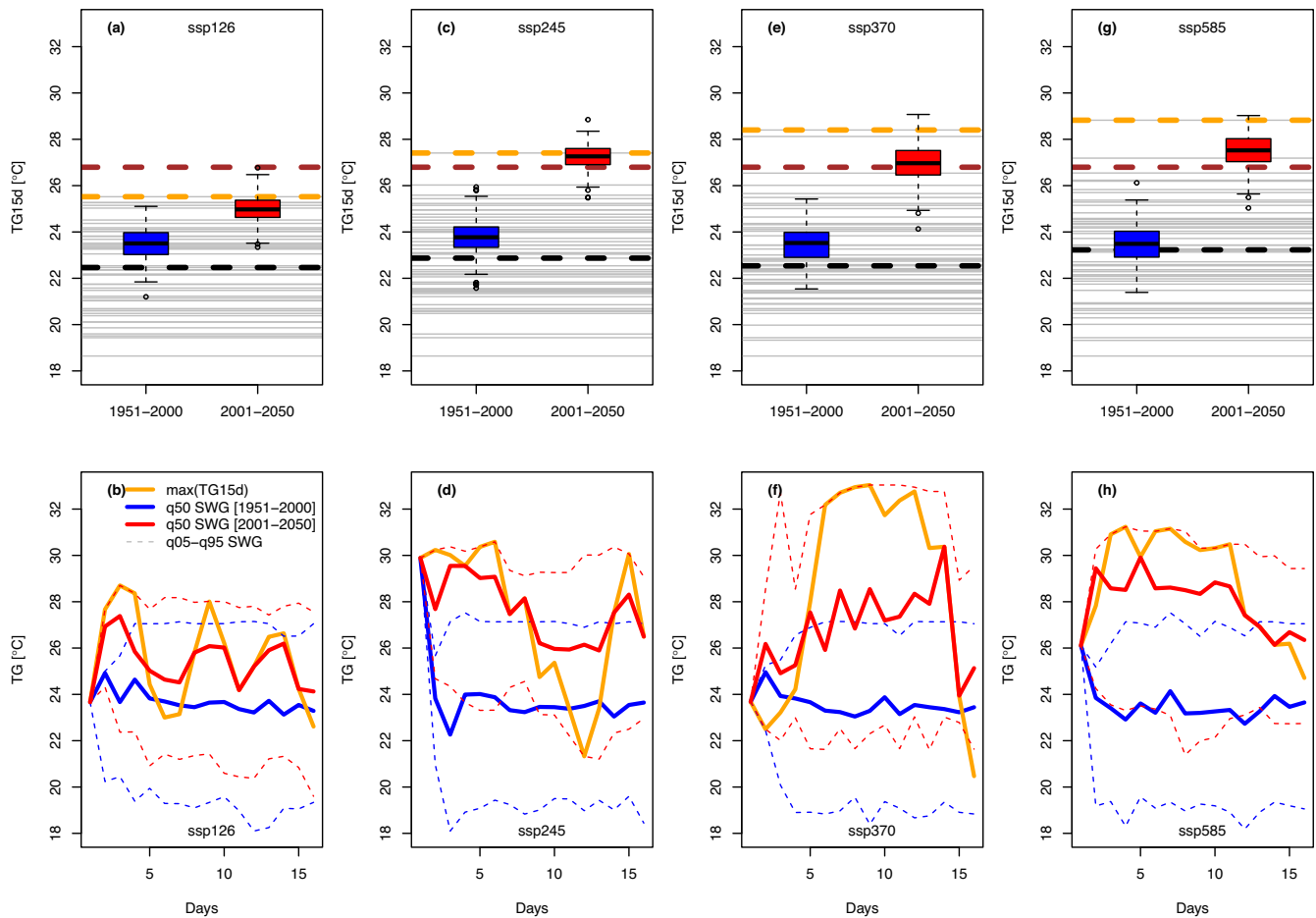
Fig. 2 SWG simulations of TG15d from IPSL model data. Upper panels (**a, c, e, g**): Boxplots of 200 SWG simulated mean 15-day temperatures, with analogs in 1951–2000 (blue boxplots) and 2001–2050 (red boxplots) in the IPSL model data for the four SSP scenarios (see Methods Section on simulation protocol). The boxplot definition is the same as in Fig. 1. Horizontal lines represent TG15d in each IPSL model SSP simulation (obtained from Fig. 1a). The dashed black line is the median, for each SSP simulation. The horizontal brown dashed line is the value that was observed in 2003, from ERA5 (Fig. 1a). Lower panels (**b, d, f, h**): time variations of the simulated temperatures with the SWG. The blue lines are for SWG simulations with analogs in 1951–2000. The red lines are for SWG simulations with analogs in 2001–2050. The thick continuous lines represent the median of 200 simulations. The dashed lines are the daily 5th and 95th quantiles of the 200 simulations. The thick orange lines are the daily variations for the record year identified in the upper panels.

the SWG simulations and analogs in 2001–2050. The occurrence of a heatwave that exceeds the 2003 record value (red dash-dotted lines) by almost 2 °C in the 2001–2050 SWG simulations is possible, except in the SSP1-2.6 scenario (because the most extreme TG15d in the IPSL SSP1-2.6 simulation is lower than the TG15d in 2003 in ERA5).

Daily time series of simulated temperatures with SWG are shown in the lower panels of Fig. 2. This illustrates the range of daily variations of temperature. The initial conditions are chosen in 2001–2050 for all SWG simulations. This explains why the simulated TG values with analogs in 1951–2000 sometimes decrease after the second day (e.g. in SSP2-4.5 and SSP5-8.5). The simulations with analogs in 2001–2051 mostly stick to the upper quantile, leading to a lower variance.

We investigate the atmospheric circulation patterns during the 15-day heatwaves, for the IPSL model. Figure 3 (first column) shows the 15-day average of SLP and SLP anomalies during the most extreme heatwaves in 2001–2050 detected in each scenario simulation. The four identified extreme heatwaves occurred between 2033 (SSP5-8.5) and 2049 (SSP2-4.5). As expected from other studies[18,19], the four record heatwaves are characterized by strong anticyclonic conditions over Scandinavia and west of France. A cyclonic SLP anomaly is detected over France, which is reminiscent of a cut-off low that advects warm air into France

from North Africa. This can be seen in the supplementary movie, which shows how a cyclonic anomaly interacts with the Scandinavian anticyclone during an episode of high TG15d, contributing to an increase in temperature. This combination of general anticyclonic conditions and a cut-off low was observed in the summer of 2022 in France (Supplementary material). The stochastic simulations with analogs in 1951–2000 (Fig. 3, central column) exhibit similar circulation patterns, with this combination of anticyclonic conditions and a cut-off low. The stochastic simulations with analogs in 2001–2050 (Fig. 3, right column) are very similar to the record events (left column) because the simulations can select analogs during those events. The atmospheric structures in the North West Atlantic do not contribute to the heatwave in France, as analogs that are computed on a smaller region lead to similar TG15d values (Supplementary Fig. 2).

The similarities of the atmospheric patterns over the North Atlantic during the most extreme heatwaves across the four SSP scenarios (in one model) suggest that "ultimate" heatwaves that are likely to strike Ile-de-France are associated with this combination of an extended blocking (which can last for several weeks) leading to clear skies and low winds, and a cut-off low (whose lifetime is just a few days) that pumps warm air into Europe. The heatwaves that occurred in France in the 21st century are examples of this combination.
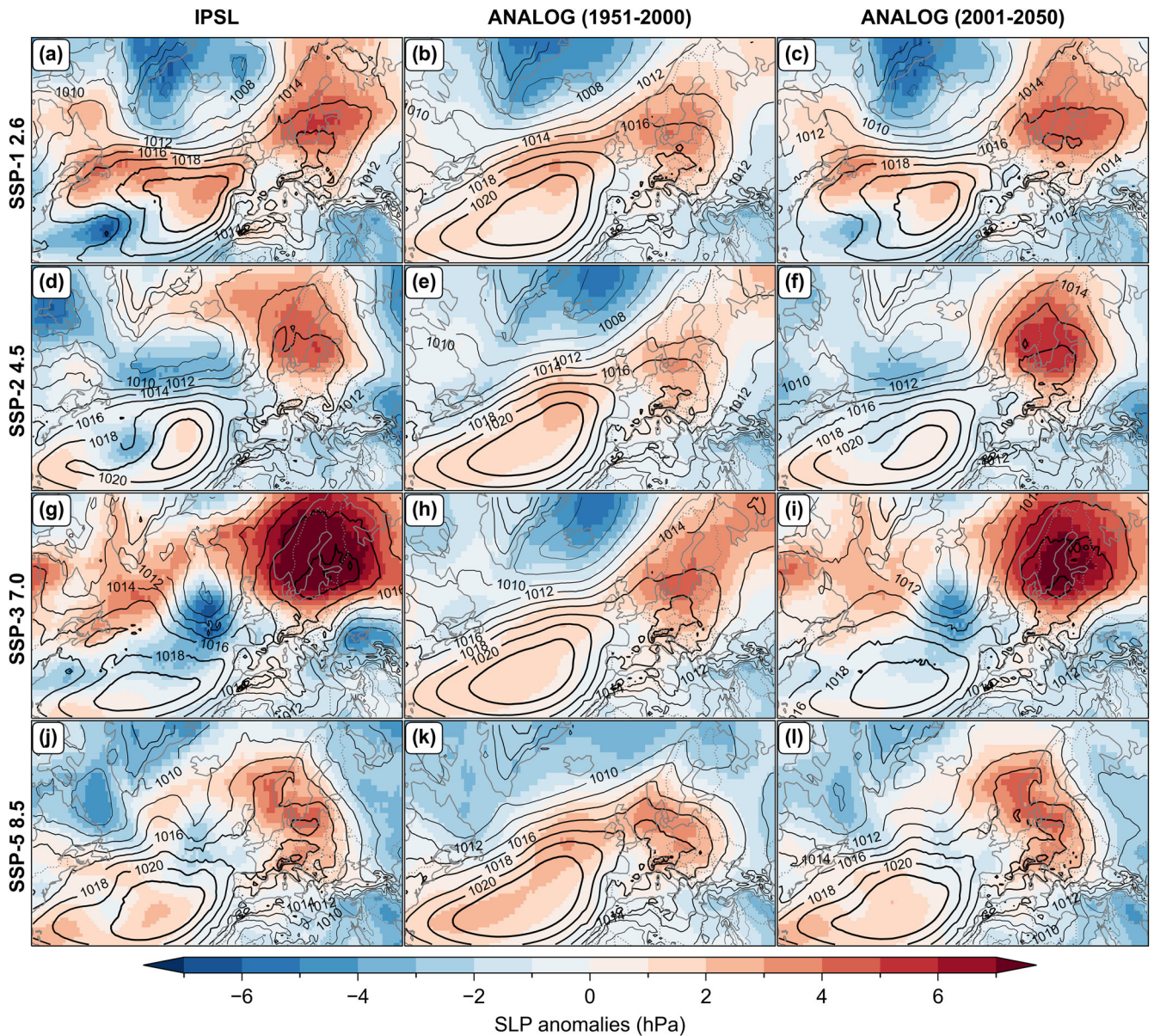
Fig. 3 North Atlantic atmospheric patterns during TG15d events in the Paris area. SLP maps over the North Atlantic region during the most intense 15-day heatwaves detected in four IPSL ssp simulations (left panels **a**, **d**, **g**, **j**). Extreme simulations with analogs in 1951–2000 (central panels **b**, **e**, **h**, **k**). Extreme simulations with analogs in 2001–2050 (right panels **c**, **f**, **i**, **l**). Colors represent SLP anomalies (hPa). Isolines represent SLP (hPa).

## Stochastic simulations with CMIP6 models

The SWG simulations are applied to other CMIP6 simulations, to test the robustness of the results reported in Fig. 2 and the IPSL model. The procedure is the same as for the IPSL model (see Methods).

There is a large variability of extreme heatwave SWG simulations across CMIP6 models (Fig. 4). The value of extremes often increases by more than 4 °C between 1951–2000 and 2001–2050. The value of the 2003 observed record is reached for two models (CMCC and MIROC) with the analogs in 1951–2000, and starting with an initial condition in 2001-2050. The MIROC model is the only one for which the record value of 26.8 °C (observed in 2003 in ERA5) is almost reached in the historical period (26.6° in 1984 in the MIROC calendar). The initial condition leading to the record in 2001–2050 (in 2043 for SSP5-8.5) is similar to the initial condition leading to the record in 1984, in the MIROC model years. This explains the apparent outlier of the temperature distribution for

SSP5-8.5 with the MIROC model (lower right in Fig. 4d). The 2003 value (of ERA5) is exceeded for most models in 2001-2050, for all initial conditions in CMIP6 models.

The mean and median temperatures of TG15d marginally increase with the SSP scenario by 2050 (Fig. 1b for IPSL model). Likewise, the most extreme values that are simulated by the SWG only slightly increase from SSP1-2.6 to SSP5-8.5, when pooling all models together, from 23.6 °C to 24 °C. This increase is smaller than the intermodel standard deviation ($\approx$ 1.2 °C). Some models allow simulating the highest TG15d from "weaker" SSP scenarios (e.g., CMCC, EC-Earth). This is due to the fact that those model simulations (with SSP1-2.6) yield record shattering TG15d events, which exceed the values obtained in 2001–2050 for the other scenarios.

The SLP maps of CMIP6 simulations are shown in Supplementary Figs. 4–14. A few CMIP6 models yield the atmospheric circulation scenario that was described for the IPSL model.
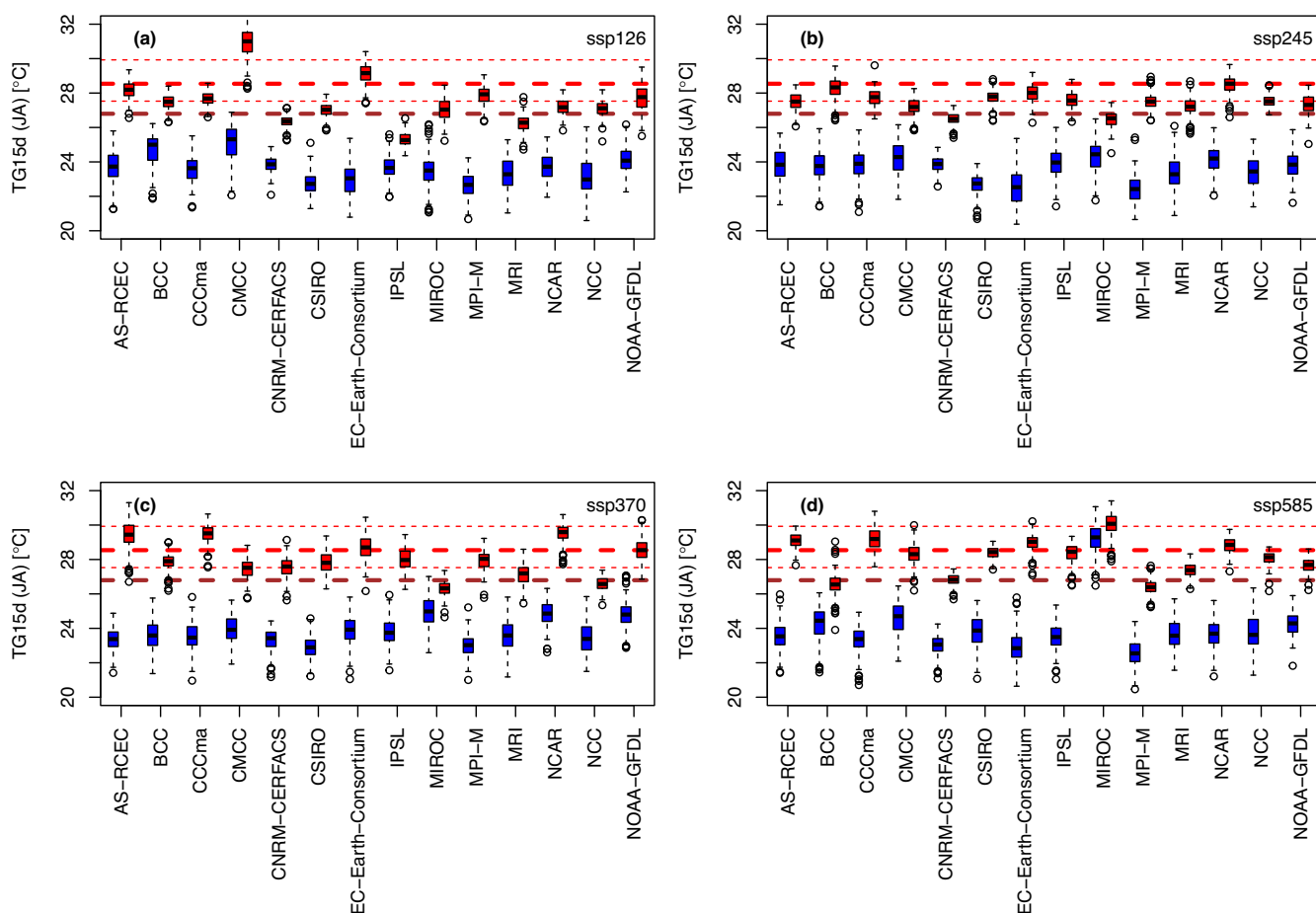
Fig. 4 Boxplots of maximum 15-day averages, starting on the most extreme heatwave in 2001-2050, detected in each CMIP simulation. Blue boxplots are for analogs in 1951–2000. Red boxplots are for analogs in 2001–2050. The boxplot definition is the same as in Fig. 1. Thick horizontal red lines represent estimates of return levels with a return period of 100 years, with a multi-model Generalized Extreme Value (GEV) estimate (see section ExtremeValueAnalysis). The dashed horizontal red lines represent the 95% confidence interval of the return value estimates. Brown dashed lines represent the value in 2003 from the ERA5 reanalysis.

We compare those SWG simulation results with a multi-model estimate of extreme values of temperature obtained from a fit to a non-stationary Generalized Extreme Value (GEV) distribution (see Section ExtremeValueAnalysis). This comparison is done to check the robustness of extreme TG15d value ranges. Most CMIP6 models provide estimates that are close to GEV return levels (red lines, see Section ExtremeValueAnalysis) with a return period of 100 years. A few CMIP6 models exceed the GEV upper estimate by almost 1 °C.

DISCUSSION

This study is an improvement over existing reports on the risk of heatwaves from climate projections[4], as we use state-of-the-art bias correction methods, and a large set of CMIP6 simulations. We generalize the results of[11] by considering climate change. Rather than simulating many "normal" summers and extracting the hottest, our approach directly simulates many extremely hot summers. The computing efficiency makes this approach appealing: simulating 10^4 centennial heatwaves (just over France) with general circulation models would require more than 100 times the volume of available CMIP6 data. We verified that the simulation approach is robust to the choice of parameters like the choice of region for analogs (Supplementary Figures 1 and 2).

This study is not a forecast for July-August 2024 in Paris, but a risk assessment of extreme heatwaves in a changing climate. Temperatures that exceed the 2003 record by $\approx 4°C$ after 2020 in

Ile-de-France are possible. Model simulations suggest that such records could also be shattered in the 2020-2050 decades.

This study comes with caveats. Most selected initial conditions occur after 2020 in the CMIP6 simulations, due to the increase of temperature in the 2001-2050 period. This does not change the main message of the paper that the 2003 record can be broken, with the atmospheric circulation scenario that we identified, and which is hardly possible in 1951–2000. No local physical processes are considered in these simulations. Soil moisture or atmospheric humidity could also be used to constrain analogs, but these quantities are not always available on a daily basis for the CMIP6 simulations we used. Taking such processes into account is possible with our approach, and could potentially enhance the heatwaves. Therefore, our estimates can be considered as lower bounds that are based mainly on atmospheric dynamics properties.

This paper takes information from 4 scenarios $\times$ 14 models $= 56$ extreme heatwaves of 15 days (TG15d) from CMIP6 simulations. We have produced an ensemble of $200 \times 56 \approx 10^4$ centennial heatwaves for the 2001–2050 decades. Those heatwaves exceed the 2003 record values in France and the record values in individual CMIP6 simulations.

Such climate events pose a serious health threat, especially for social events where crowds gather outdoors, like in the Olympic games. Those heat events seem to occur with anticyclonic conditions, leading to low surface winds, which enhances the health threat, as air pollutants are not dispersed[20]. The addition of

a cut-off low that transports warm air from North Africa can increase the temperature in a short time. The health risk associated with high temperatures is documented in France[21,22]. It can be expected that the accumulated risk is proportional to the length of the heatwaves[23]. Heatwaves of 15 days or more have occurred in Paris (2003), Russia (2010) or Western Canada (2021), and are therefore physically plausible.

Recent initiatives from the City Council of Paris have been undertaken for long-term urban planning[24]. The results of this paper complement Paris reports for a closer horizon.

The domain of application of our simulation approach obviously goes beyond the Paris Olympics in 2024 (or any major outdoors sports event in that region). It could be adapted to other regions of the world, where surface temperature is linked to atmospheric circulation. Such an approach can be used to design so-called storylines of events[25,26], for impact models or for communication on extreme events in a changing climate.

METHODS

Data and bias correction
We use the simulations of 14 CMIP6 models (out of 31 models)[14] (see Supplementary Table 1) and four shared socio-economic pathways (SSP) scenarios [27] (SSP1-2.6, 2-4.5, 3-7.0 and 5-8.5). The criterion to retain these models is their availability on an Earth System Grid Federation (ESGF) server for the four SSP scenarios on daily increments. A data quality check is also performed on the available files. The historical simulations cover 1850-2014. The scenario (SSP) simulations cover 2015-2100. We extract the model gridpoints that cover continental France. For simplicity, we take one simulation for each model (some models provide ensembles) and visually check that this choice samples the overall spread of all simulations.

The multivariate bias correction method R^2D2[15] is used to correct the bias of the marginals and the dependency structure of the temperature and precipitation, with respect to the SAFRAN reanalysis[28] (≈ 8 km of horizontal resolution). The R^2D2 method is based on the CDF-t method[29], which takes into account the climate change signal. The method is trained on the 1976-2005 period, and applied between 1850 and 2100 on moving periods of 10 years. The bias correction procedure acts on the whole probability distribution. Therefore, the variance is also corrected (as well as higher order moments).

We compute the spatial average of the mean daily temperature over Ile-de-France. The 2001–2050 decades stand across the historical and scenario range. We aggregate the historical (1850–2014) and scenario (2015–2100) simulations, to obtain $4 \times 14 = 56$ time series of daily temperatures.

Circulation analogs are computed from SLP fields from the same models over the North Atlantic region (80W–50E; 22.5N–70.5N). Other fields (e.g. geopotential height at 500hPa) could be used in principle, but only SLP is available on a daily basis for the 14 models identified for temperature. Analogs were also computed on a smaller region (30W–20E; 40N–60N), in order to verify the robustness of results to the choice of the region. Analogs were computed with time embeddings of 1 day and 3 days.

Since the bias correction cannot be done with the SAFRAN reanalysis (which covers only France), we consider the ERA5 reanalysis[17] and use the CDF$-t$ univariate bias correction method[29] for SLP. The spatial correlation between the corrected SLP and "raw" SLP was high (i.e. the spatial patterns do not change much)

For comparison purposes with CMIP6, we extract the mean temperature over Ile-de-France for the ERA5 reanalysis (1950-2021)[17] from the climate explorer tool (https://climexp.knmi.nl/).

Heatwave identification
For each year, we consider moving 15-day periods between July 1st and August 31st. In each temperature time series (for each model, for each scenario), we determine the warmest yearly 15-day spell (TG15d). These values are reported in Fig. 1. Each temperature value obviously corresponds to a different starting date. We then determine the first day of the moving 15-day hottest spells. Hence, rather than starting on the 26th of July (the beginning of the 2024 Olympics), we start on the date determined by the warmest 15-day spell in July-August. This is close to the procedure for ensemble boosting simulations[30]. The paper then focuses on the most intense TG15d in 2001-2050.

Stochastic weather generator (SWG) and importance sampling
We use the approach of[11], which emulates temperature variations with a stochastic weather generator (SWG)[31] based on analogs of atmospheric circulation. This corresponds to a Markov chain of temperature, with latent states of the atmospheric circulation. The general procedure is summarized as follows. For each day in 1950-2050, we consider its best 20 analogs of SLP. Simulations are initialized on a summer day.

1. We randomly select one SLP analog day, with sampling weights that favor higher temperatures and a time progression.
2. The next day the sampled analog is selected.
3. Steps 1 and 2 are repeated 14 times to get a 15-day trajectory.
4. Steps 1 to 3 are repeated 200 times to get 200 trajectories of 15 days.

This corresponds to a procedure of *importance sampling*[11]. If the weights are uniform, this is equivalent to a normal emulator of temporal sequences[12]. The parameter that controls the weights towards high temperatures is $a_T = 0.4$, which roughly corresponds to simulating centennial events[11].

Experimental set-up of simulations
We simulate heat waves between 2001 and 2050, which are the five decades that roughly bracket 2024. We initiate heatwaves in this period from CMIP6 simulations, and evaluate the role of climate change in heatwave that "could have been", in historical and scenario configurations, with a constraint on the atmospheric circulation.

We compute SLP analogs of 1900–2100 in 1951–2000 (historical period) and 2001–2050 (scenario period). This is done for the four scenarios and 14 CMIP6 models. This helps to sample low-frequency variability, since all models yield different ocean configurations.

For the paper, the initial conditions of the SWG simulations are the first day of the warmest 15-day period (in July and August, TG15d), for each year (between 2001 and 2050), each CMIP6 model and each SSP scenario. We simulate 200 trajectories for each initial condition. An illustration of such simulations with data from the IPSL model is provided in Figs. 2 and 3. A synthesis with all 14 CMIP6 model data is shown in Fig. 4.

For verification purposes, the SWG simulations from the IPSL model were computed with analogs covering a smaller region than the North Atlantic. This is reported in the Supplementary Information.

Extreme value analysis
An upper bound estimate of the return value of a 15-day heatwave is inferred with the method of[32], based on Generalized Extreme Value (GEV) modeling[16]. A multi-model synthesis of non-stationary GEV parameters from each climate model is used as prior. A posterior is derived using Bayesian techniques based on SAFRAN reanalysis statistics, considered as a reference. This approach allows us to have a non-stationary GEV model covering the period 1850–2100 for each

scenario, and constrained by the reference reanalysis. With this procedure, we obtain a statistical estimate of return levels associated with return periods of 100 years. We also compute 95% credible intervals on empirical quantiles of the return level estimates obtained from the Markov Chain Monte Carlo simulations that are performed in the Bayesian techniques.

DATA AVAILABILITY

Data availability: ERA5 reanalysis temperature data is available from the Climate Explorer tool https://climexp.knmi.nl/start.cgi. CMIP6 data without bias corrections (temperature, S.L.P.) is available from the Earth System Grid Federation (ESGF) node https://esgf-node.ipsl.upmc.fr/projects/cmip6-ipsl/. Bias-corrected data (temperature, S.L.P.), S.L.P. analogs, and SWG simulations are available upon request to the corresponding author (P.Y.).

CODE AVAILABILITY

Code availability: SWG code is available on github: https://github.com/pascalyiou/UNCLE-with-Analog-SWG. The bias correction code is available on github: https://github.com/yrobink/SBCK.

REFERENCES

1. Schaer, C. & Jendritzky, G. Climate change: Hot news from summer 2003. *Nature* **432**, 559–560 (2004).
2. Kovats, R. S. & Hajat, S. Heat stress and public health: a critical review. *Annu. Rev. Public Health* **29**, 41–55 (2008).
3. Van Vliet, M. T., Sheffield, J., Wiberg, D. & Wood, E. F. Impacts of recent drought and warm years on water resources and electricity supply worldwide. *Envir. Res. Lett.* **11**, 124021 (2016).
4. Seneviratne, S. et al. In *Weather and Climate Extreme Events in a Changing Climate* (eds Masson-Delmotte, V. et al.) *Climate Change 2021: The Physical Science Basis. Contribution of Working Group I to the Sixth Assessment Report of the Intergovernmental Panel on Climate Change* 1513–1766 (Cambridge University Press, Cambridge, United Kingdom and New York, NY, USA, 2021). Type: Book Section.
5. Watts, J. Olympic athletes and volunteers in Tokyo 'tortured' by hottest Games ever. *The Guardian* https://www.theguardian.com/environment/2021/aug/05/olympic-athletes-and-volunteers-in-tokyo-tortured-by-heat (2021).
6. Kakamu, T., Wada, K., Smith, D. R., Endo, S. & Fukushima, T. Preventing heat illness in the anticipated hot climate of the Tokyo 2020 Summer Olympic Games. *Environ. Health Prev. Med.* **22**, 68 (2017).
7. Vanos, J. K. et al. Planning for spectator thermal comfort and health in the face of extreme heat: The Tokyo 2020 Olympic marathons. *Sci. Total Environ.* **657**, 904–917 (2019).
8. National Academies of Sciences Engineering and Medicine (ed.) *Attribution of Extreme Weather Events in the Context of Climate Change* (The National Academies Press, Washington, DC, 2016). www.nap.edu/catalog/21852/attribution-of-extreme-weather-events-in-the-context-of-climate-change.
9. Ragone, F., Wouters, J. & Bouchet, F. Computation of extreme heat waves in climate models using a large deviation algorithm. *Proc. Nat. Acad. Sci.* **115**, 24–29 (2018). ISBN: 0027-8424 Publisher: National Acad Sciences.
10. Ragone, F. & Bouchet, F. Rare event algorithm study of extreme warm summers and heatwaves over Europe. *Geophys. Res. Lett.* **48**, e2020GL091197 (2021).
11. Yiou, P. & Jézéquel, A. Simulation of extreme heat waves with empirical importance sampling. *Geosci. Model Dev.* **13**, 763–781 (2020).
12. Yiou, P. AnaWEGE: a weather generator based on analogues of atmospheric circulation. *Geosci. Model Dev.* **7**, 531–543 (2014).
13. Yiou, P. et al. Analyses of the Northern European summer heatwave of 2018. *Bull. Am. Meteorol. Soc.* **101**, S35–S40 (2020).
14. Eyring, V. et al. Overview of the Coupled Model Intercomparison Project Phase 6 (CMIP6) experimental design and organization. *Geosci. Model Dev.* **9**, 1937–1958 (2016).
15. Vrac, M. & Thao, S. R 2 D 2 v2. 0: accounting for temporal dependences in multivariate bias correction via analogue rank resampling. *Geoscientific Model Development* **13**, 5367–5387 (2020).
16. Coles, S. *An introduction to statistical modeling of extreme values* Springer series in statistics (Springer, London, New York, 2001).
17. Hersbach, H. et al. The ERA5 global reanalysis. *Quat. J. Roy. Met. Soc.* **146**, 1999–2049 (2020). ISBN: 0035-9009 Publisher: Wiley Online Library.
18. Quesada, B., Vautard, R., Yiou, P., Hirschi, M. & Seneviratne, S. I. Asymmetric European summer heat predictability from wet and dry southern winters and springs. *Nature Climate Change* **2**, 736–741 (2012).
19. Mueller, B. & Seneviratne, S. Hot days induced by precipitation deficits at the global scale. *Proc. Natl. Acad. Sci. USA* https://doi.org/10.1073/pnas.1204300109 (2012).
20. Pirard, P. et al. Summary of the mortality impact assessment of the 2003 heat wave in France. *Eurosurveillance* **10**, 7–8 (2005).
21. Vandentorren, S. et al. Mortality in 13 French cities during the August 2003 heat wave. *Am. J. Public Health* **94**, 1518–1520 (2004).
22. Pascal, M. et al. Heat and cold related-mortality in 18 French cities. *Environ. Int.* **121**, 189–198 (2018).
23. Anderson, G. B. & Bell, M. L. Heat waves in the United States: mortality risk during heat waves and effect modification by heat wave characteristics in 43 US communities. *Environ. Health Perspect* **119**, 210–218 (2011).
24. Florentin, A. & Lelievre, M. Mission d'information et d'évaluation du Conseil de Paris Paris à 50 degrés: s'adapter aux vagues de chaleur. Tech. Rep., Paris City Council https://cdn.paris.fr/paris/2023/05/23/mie-paris-a-50-Moer.pdf (2023).
25. Shepherd, T. G. Storyline approach to the construction of regional climate change information. *Proc. R. Soc. Lond. A* **475**, 20190013 (2019).
26. Sillmann, J. et al. Event-based storylines to address Climate risk. *Earth's Future* **9**, e2020EF001783 (2021).
27. Riahi, K. et al. The Shared Socioeconomic Pathways and their energy, land use, and greenhouse gas emissions implications: an overview. *Glob. Environ. Change* **42**, 153–168 (2017). ISBN: 0959-3780 Publisher: Elsevier.
28. Quintana-Segui, P. et al. Analysis of near-surface atmospheric variables: validation of the SAFRAN analysis over France. *J. Appl. Meteorol. Climatol.* **47**, 92–107 (2008).
29. Michelangeli, P.-A., Vrac, M. & Loukos, H. Probabilistic downscaling approaches: application to wind cumulative distribution functions. *Geophys. Res. Lett.* **36** (11) (2009).
30. Gessner, C., Fischer, E. M., Beyerle, U. & Knutti, R. Very rare heat extremes: quantifying and understanding using ensemble reinitialization. *J. Clim.* **34**, 6619–6634 (2021).
31. Ailliot, P., Allard, D., Monbet, V. & Naveau, P. Stochastic weather generators: an overview of weather type models. *Journal de la Société Française de Statistique* **156**, 101–113 (2015).
32. Robin, Y. & Ribes, A. Nonstationary extreme value analysis for event attribution combining climate models and observations. *Adv. Stat. Climatol. Meteorol. Oceanogr.* **6**, 205–221 (2020).

AUTHOR CONTRIBUTIONS

Authors contributions: P.Y. designed the experiments. Y.R. computed the bias CMIP6 correction and GEV estimates. R.N. made the animated gifs. All authors contributed to the writing of the manuscript.

COMPETING INTERESTS

The authors declare no competing interests.

ADDITIONAL INFORMATION

Supplementary information The online version contains supplementary material available at https://doi.org/10.1038/s41612-023-00500-5.

Correspondence and requests for materials should be addressed to Pascal Yiou.

Reprints and permission information is available at http://www.nature.com/reprints

Publisher's note Springer Nature remains neutral with regard to jurisdictional claims in published maps and institutional affiliations.